Targeted Nanoparticle-Based Therapy Using Betaine-Conjugated Gold Nanoparticles for Reducing Inflammation and Modulating Immune Response in Heatstroke-Induced Mice

Alireza Loghmani[1] ✉ iD, Mohammad Kamalpour[2] iD, Mohammad Amrollahi-Sharifabadi[2] iD,
Mohammad Bahrami Tapehbour[3] iD

1. Department of Pathobiology, Faculty of Veterinary Medicine, Lorestan University, Khorramabad, Iran
2. Department of Basic Sciences, Faculty of Veterinary Medicine, Lorestan University, Khorramabad, Iran
3. Department of Anatomy and Embryology, Faculty of Veterinary Medicine, Lorestan University, Khorramabad, Iran

Article Info

Abstract

Background & Objectives: The present study investigates the therapeutic potential of betaine-conjugated gold nanoparticles (AuNPs) in treating inflammation induced by heatstroke. While heatstroke is characterized by elevated body temperature and severe inflammation, which can lead to organ dysfunction, conventional treatments, such as cooling and supportive care have not been successful in preventing long-term damage. AuNPs function as targeted carriers for the delivery of bioactive agents, such as betaine, to inflamed tissues. Using a murine model of heatstroke, we assessed the effects of AuNPs, betaine, and their combination on inflammation markers and cellular stress.

Materials & Methods: The experimental animals were divided into groups receiving different treatments, and various outcomes, including cytokine levels (TNF-α, IL-6, IL-10), heat shock protein (HSP70) expression, and splenocyte proliferation, were measured.

Results: The findings revealed that the combination of AuNPs and betaine significantly decreased the levels of pro-inflammatory cytokines (TNF-α and IL-6) while increasing those of the anti-inflammatory cytokine IL-10. Furthermore, the therapy reduced HSP70 expression, indicating lowered cellular stress in the AuNP-betaine group. Moreover, treatment with AuNP-betaine significantly enhanced lymphocyte proliferation, suggesting improved immune function under heatstroke conditions.

Conclusion: Our findings highlight the promise of betaine-conjugated AuNPs as an innovative therapeutic approach in reducing inflammation and oxidative stress associated with heatstroke. The synergistic effects of nanotechnology and bioactive substances in modulating inflammatory pathways can be a promising strategy for managing heat-related inflammatory conditions.

Keywords: Heatstroke, Betaine, Gold Nanoparticle (AuNP), Inflammation, Heat Shock Protein (HSP70).

Introduction

Heatstroke is a critical and potentially life-

✉**Corresponding Author: Loghmani Alireza,**
Department Pathobiology, Faculty of Veterinary Medicine, Lorestan University, Khorramabad, Iran.
Email: Loghmani.al@lu.ac.ir

threatening condition marked by extreme hyperthermia and widespread inflammation, which can lead to organ failure. This severe medical emergency typically arises from prolonged exposures to high temperatures and can trigger severe complications, including

319

heat-related inflammatory reactions, oxidative damage, and extensive tissue harm. Heatstroke affects millions worldwide, with particularly high incidence in regions experiencing extreme temperatures. According to recent data, over 70,000 deaths were attributed to heatwaves globally in the last decade, highlighting the critical need for innovative treatments (1). Heatstroke occurs when the body's core temperature exceeds 40°C (104°F), leading to hyperthermia and significant inflammation. This condition results in an excessive release of pro-inflammatory cytokines, including interleukin-1β (IL-1β), interleukin-6 (IL-6), and tumor necrosis factor-α (TNF-α) (2). Research has shown that oxidative stress dramatically enhances the inflammatory response during heatstroke, resulting in extensive cell death and tissue damage in vital organs, including the liver, kidneys, and brain (3).

Although quick cooling and supportive care remain the usual treatments for heatstroke (4), there exists a pressing necessity for effective drug interventions to reduce inflammation and prevent organ damage. In recent years, there has been significant interest in discovering new therapies that target the inflammatory pathways involved in heatstroke (5). Inflammatory responses in heatstroke are primarily driven by the release of pro-inflammatory cytokines, such as IL-6, TNF-α, and IL-1β. These molecules exacerbate oxidative stress by generating reactive oxygen species (ROS), which further damage cellular proteins, lipids, and DNA, leading to organ dysfunction.

Research has demonstrated that oxidative stress dramatically enhances the inflammatory response during heatstroke, resulting in increased cell death and tissue damage in vital organs, including the liver, kidneys, and brain (6). Furthermore, nanotechnology presents promising opportunities for creating targeted treatment methods for various health issues, particularly inflammatory disorders. Among these, gold nanoparticles (AuNPs) stand out

as remarkably adaptable and biocompatible systems. Their adjustable size, surface characteristics, and ability to transport bioactive substances directly to damaged areas make them particularly valuable (7, 8).

Recent research has demonstrated that AuNPs can effectively reduce inflammation and oxidative damage in multiple disease models (9, 10). Moreover, betaine, a naturally occurring substance recognized for its antioxidant and anti-inflammatory properties, has demonstrated potential in reducing inflammatory reactions and providing protection against tissue damage (11). This research focuses on exploring the anti-inflammatory effects of AuNP carriers when combined with betaine, using a mouse model that simulates heatstroke conditions. By combining the distinct properties of AuNPs with the therapeutic advantages of betaine, this study aims to elucidate the effectiveness of nanoparticle-driven treatments in reducing inflammation and oxidative damage induced by heatstroke.

Material and Methods
Synthesis of Betaine-Loaded AuNPs
Initially, a 50 mL water-based mixture of AuNPs containing 2.5 mg of AuNPs was synthesized following previously established protocols (12). Subsequently, a 100 mL solution of 1 mg betaine dissolved in CH_3OH was prepared. In parallel, an aqueous solution of either 13.3 mg or 26.6 mg of mPEG thiol (5 kDa) was formulated in 1.0 mL of water. Following preparation, the solutions of AuNPs, betaine, and mPEG thiol were combined and subjected to continuous stirring for 48 hours at room temperature.

To purify the product, the removal of unbound betaine and mPEG thiol was accomplished through centrifugation using an Eppendorf Centrifuge 5810 R equipped with a rotor diameter of 10 cm, operating at 14,000 rpm (10,956 x g) for 20 minutes at room temperature. Following

centrifugation, the supernatant was carefully removed via pipette, and the nanoparticle pellet was resuspended in water. This centrifugation and resuspension process was repeated three times to ensure complete removal of unbound materials. The final residue was resuspended in 1.0 mL of water, yielding betaine-loaded AuNPs. A parallel synthesis was conducted using 2 mg of betaine and 13.3 mg of mPEG thiol to generate a sample designated as Au-Betaine. Four batches of each sample were synthesized for further characterization.

Characterization of Gold Nanoparticles (AuNPs) and Their Betaine Conjugates

Transmission Electron Microscopy (TEM)

For the purpose of evaluating the morphology and size of AuNPs, Transmission Electron Microscopy (TEM) analysis was conducted. The sample was prepared by depositing a small drop of the nanoparticle suspension (1 mg/mL) onto a carbon-coated copper grid, which was then allowed to air dry. The prepared samples were subsequently examined using a JEOL JEM-2100 TEM operated at 100 kV. Image analysis software was employed to assess size distribution and particle morphology. The analysis revealed that the particles predominantly exhibited a spherical form, and the average diameter was determined through the analysis of multiple images.

Dynamic Light Scattering (DLS) Method

The characterization of hydrodynamic diameter and polydispersity index (PDI) of AuNPs was performed using Dynamic Light Scattering (DLS). The nanoparticle samples were diluted in deionized water to achieve a concentration of 0.01 mg/mL and transferred into a clean quartz cuvette. DLS measurements were performed utilizing a Zetasizer Nano (Malvern Instruments) at an ambient temperature of 25°C. The measurements yielded data on size distribution based on intensity, while the PDI values provided information regarding the uniformity of the particle sizes. Notably, a PDI value lower than 0.2 indicated that the AuNPs

were monodispersed. All measurements were conducted in triplicate prior to calculating the average size.

UV-Visible Spectroscopy

The formation of AuNPs was confirmed through UV-Visible Spectroscopy, which enabled the detection of the surface plasmon resonance (SPR) characteristics of AuNPs. After the AuNP suspension was diluted to 0.1 mg/mL in deionized water, researchers measured the absorbance spectrum using a UV-Vis spectrophotometer over a wavelength range of 400–700 nm. The SPR peak, typically observed at approximately 520 nm, confirmed the presence of AuNPs. A sharp and intense peak indicated that the nanoparticles were monodisperse and remained free from aggregation.

Fourier Transform Infrared Spectroscopy (FTIR) Procedure

To confirm the successful conjugation of betaine onto AuNPs, researchers employed Fourier Transform Infrared Spectroscopy (FTIR). The lyophilized AuNP-betaine conjugates were mixed with potassium bromide (KBr) and subsequently compressed into pellets. FTIR spectra were obtained over the range of 4000 to 400 cm^{-1}.

Induction of Heatstroke Model Experimental Setup

Mice were randomly divided into the following groups (n=10 per group):
1. Control: Mice maintained at ambient temperature (no heat exposure)
2. Heatstroke: Mice subjected to elevated temperatures without treatment
3. Heatstroke + AuNPs: Mice treated with AuNPs (5 mg/kg)
4. Heatstroke + Betaine: Mice administered betaine (20 mg/kg)
5. Heatstroke + AuNP-Betaine: Mice treated with AuNP-betaine conjugates (5 mg/kg AuNPs, 20 mg/kg betaine)

Heat Exposure Method

Heatstroke was induced by placing the mice

in an environmentally controlled chamber maintained at 42°C with 30% humidity. The researchers continuously monitored the mice, measuring core body temperature via a rectal probe. Heat exposure continued until the core temperature reached 41.5°C, whereupon the mice were transferred to room temperature (22°C) for recovery (13, 14).

Administration of Treatment

All treatments (AuNPs, betaine, or AuNP-betaine conjugates) were administered intravenously 30 minutes before heat exposure. Control mice received an equivalent volume of saline solution.

Cytokine Assessment

Blood samples were collected via cardiac puncture 6 hours after heat exposure. Plasma levels of pro-inflammatory cytokines, specifically IL-10, IL-6, and TNF-α, were determined using enzyme-linked immunosorbent assays (ELISA) in accordance with the manufacturer's guidelines. Heat Shock Protein 70 (HSP70).

HSP70 quantification

The quantification of HSP70 was performed using a mouse HSP70-specific ELISA kit following the manufacturer's protocol. Initially, 25 µL of standards and samples were added to a 96-well ELISA plate pre-coated with an anti-HSP70 antibody and were incubated at room temperature for one hour. Following four washing cycles with wash buffer, researchers added a biotinylated detection antibody, followed by an enzyme-conjugated secondary antibody. After repeating the washing procedure, a substrate solution (TMB) was added, and the reaction was terminated after 15 minutes through the addition of a stop solution containing sulfuric acid. Subsequently, the absorbance was measured at 450 nm using a microplate reader.

MTT Assay

Following heat treatment and therapeutic intervention, splenocytes were isolated from the heat-exposed mice. The isolation process involved careful removal of the spleens, mechanical dissociation, and filtration through a mesh to obtain single-cell suspensions. After lysing red blood cells with ammonium chloride, the resulting splenocytes were resuspended in RPMI-1640 medium supplemented with 10% fetal bovine serum (FBS).

Splenocytes were seeded into 96-well plates at a density of 3×10^6 cells/mL, with 100 µL dispensed per well. The cells were then exposed to 100 µL of various treatments at a final concentration of 100 µg/mL, including AuNPs, Betaine, AuNP-betaine conjugates, and normal saline as a control. Concanavalin A (ConA) was included as a positive control to stimulate lymphocyte proliferation. The treated cells were incubated at 37°C in a 5% CO2 atmosphere for 68 hours.

Upon completion of the 68-hour incubation period, 10 µL of MTT reagent (5 mg/mL) was introduced to each well, followed by an additional 4-hour incubation to facilitate formazan crystal formation. Subsequently, 100 µL of dimethyl sulfoxide (DMSO) was added to dissolve the formazan crystals. The resulting absorbance was measured at 597 nm using an ELISA plate reader. The splenic lymphocyte proliferation index (%) was determined using the following equation:

Proliferation Index (%) = [(mean OD vaccine group - mean OD blank) / (mean OD control group - mean OD blank)] × 100

Statistical Analysis

Data are presented as mean±standard deviation (SD) unless otherwise specified. Statistical analysis was performed using one-way analysis of variance (ANOVA) to compare the means of different experimental groups. This approach was chosen because it allows for the comparison of multiple groups at once, which is essential given the different treatment groups in this study. To further assess the differences between individual groups, Tukey's post-hoc test was applied following ANOVA. Tukey's test was selected as it is commonly used for multiple

comparisons when. Statistical significance was set at a p-value of less than 0.05 (p<0.05). For graphical representation, statistical significance levels are indicated with asterisks: *p<0.05, **p<0.01, and ***p<0.001, as indicated on the error bars.

All statistical analyses were conducted using GraphPad Prism (Version 8) software, with all experiments performed in quintuplicate to ensure reproducibility and reliability of results.

Results

Transmission Electron Microscopy (TEM)

TEM imaging revealed uniformly spherical gold nanoparticles (AuNPs) with an average diameter of approximately 30 nm, as illustrated in Figure 1. The nanoparticles demonstrated good dispersion and size uniformity, confirming their spherical morphology and nanoscale dimensions.

Dynamic Light Scattering (DLS)

Analysis of the DLS intensity distribution revealed a primary peak at 35-40 nm, which indicated the predominant hydrodynamic diameter of the AuNPs (Figure 1). A secondary peak observed at 5-10 nm was attributed to minor impurities or smaller particles.

Zeta Potential Method

To assess the surface charge of AuNPs, we employed a Zetasizer Nano instrument for zeta potential measurements. We prepared a 1 mg/mL AuNP solution in deionized water and conducted measurements using a folded capillary cell at 25°C. The obtained zeta potential values indicated the surface charge and stability of AuNPs in the solution. Notably, stable colloidal AuNPs exhibited a zeta potential ranging from -30 to -40 mV, attributed to the negative surface charge resulting from citrate capping.

Fourier Transform Infrared (FTIR) Spectrum for AuNPs and AuNPs Conjugated with Betaine

The FTIR spectra revealed distinct peaks characteristic of the molecular vibrations associated with the nanoparticles and the conjugated ligand (Figure 2). We observed a prominent absorption peak at approximately 1620 cm^{-1}, which was associated with the bending vibrations of C=O groups. Additionally, a broad peak at approximately 3300 cm^{-1} was attributed to O-H stretching vibrations, likely arising from surface hydroxyl groups. Upon conjugation with betaine, the C=O peak exhibited a slight shift to 1630 cm^{-1}, suggesting changes in the local environment of the C=O bonds. Furthermore, a broader O-H stretching peak at approximately 3400 cm^{-1} corroborated the presence of hydroxyl groups and potential hydrogen bonding between betaine and AuNPs.
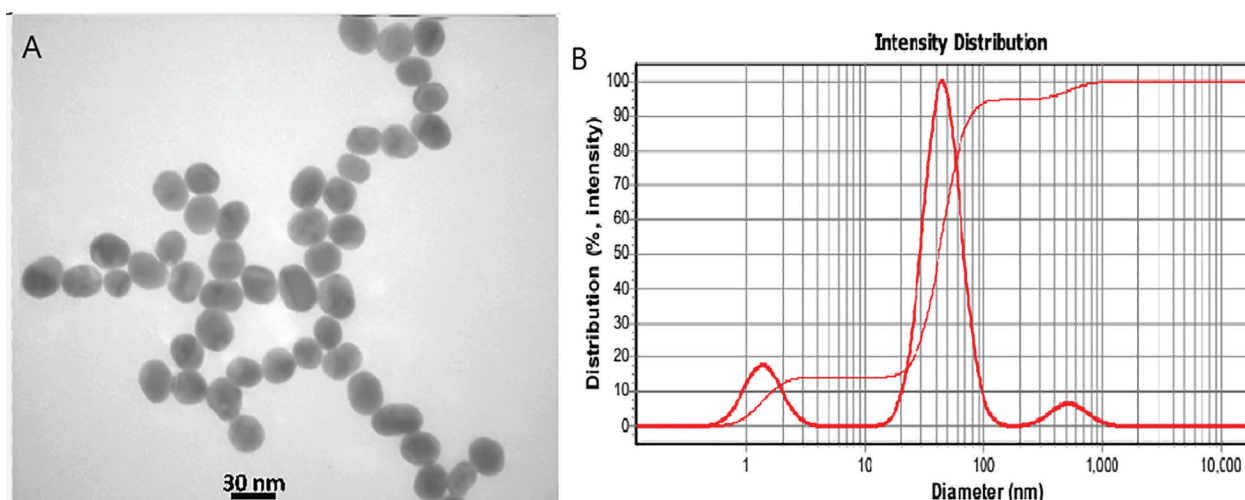

Figure 1. A: TEM image of gold nanoparticles (AuNPs) B: Dynamic Light Scattering (DLS) intensity distribution graph showing the size of gold nanoparticles (AuNPs).
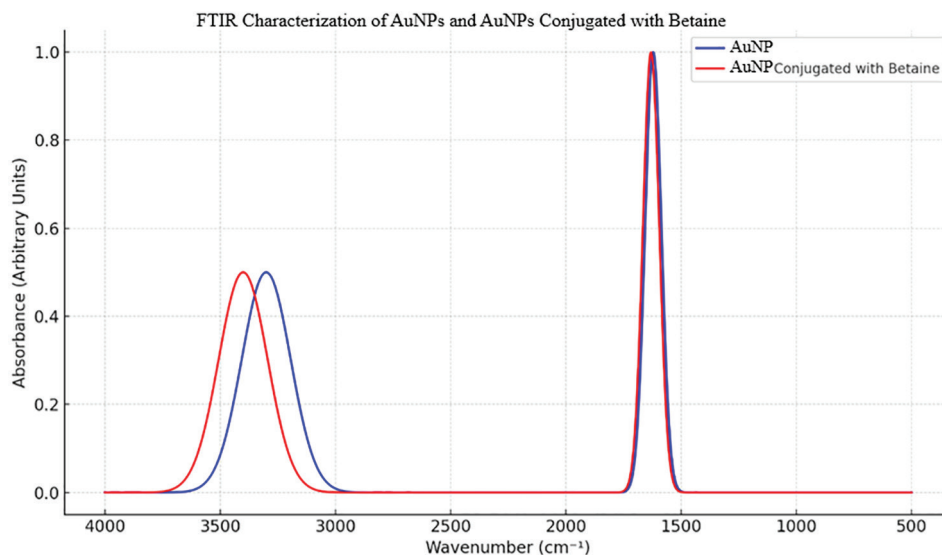
Figure 2. The plot above represents the FTIR Characterization of gold nanoparticles (AuNPs) and AuNPs conjugated with betaine. AuNPs

These results provided compelling evidence for successful conjugation of betaine to AuNPs, offering valuable insights into the structural modifications arising from the functionalization process.

Characterization Method of UV-Visible Spectroscopy

Gold nanoparticles exhibit a unique surface plasmon resonance (SPR) peak that arises from the collective oscillation of electrons at the nanoparticle surface upon illumination. This SPR peak typically manifests within the range of 520–540 nm, depending on the dimensions, morphology, and surrounding environment of the nanoparticles (Figure 3). Following the conjugation of betaine and mPEG thiol to the AuNPs, modifications in the SPR peak may occur due to changes in the local refractive index or particle aggregation. Initial Baseline Measurement (Unmodified AuNPs): We initially recorded a UV-Vis spectrum of the bare AuNPs (without betaine or mPEG thiol), wherein the SPR peak was typically observed at 520–530 nm.

Post-Conjugation Measurement (Betaine-Loaded AuNPs)

After the conjugation of betaine and mPEG thiol to the AuNPs, a subsequent UV-Vis spectrum was recorded. A shift in the SPR peak position or an increase in intensity served as indicators of successful conjugation. The comparison of spectra obtained before and after conjugation confirmed the binding of betaine and demonstrated the stabilizing effect of mPEG thiol. A slight redshift (i.e., a shift to longer wavelengths) in the SPR peak was anticipated due to the binding of betaine to the AuNP surface, which altered the local refractive index surrounding the nanoparticles. This phenomenon might also have been caused by minor aggregation or the formation of a betaine-mPEG shell around the nanoparticles.

Cytokine Analysis

Levels of TNF-α, IL-6, and IL-10 were measured to assess the inflammatory response in treated mice. Notably, the substantial reduction in TNF-α and IL-6 levels in the AuNPs + Betaine group highlighted a strong anti-inflammatory effect compared to both the control group and other treatment categories. Furthermore, the observed increase in IL-10 levels in the AuNP-Betaine group suggested enhanced anti-inflammatory properties (Chart 1).
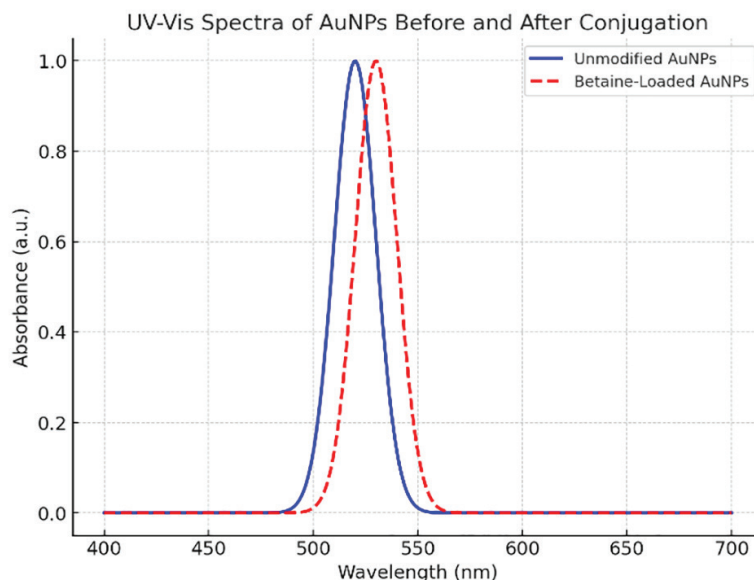
Figure 3. UV-Vis absorption spectra of gold nanoparticles (AuNPs) before and after conjugation with betaine and mPEG thiol. The blue curve represents unmodified AuNPs, exhibiting a surface plasmon resonance (SPR) peak at approximately 520 nm. Following conjugation (red dashed line), the SPR peak undergoes a bathochromic shift to approximately 530 nm, confirming successful binding of betaine to the nanoparticle surface.
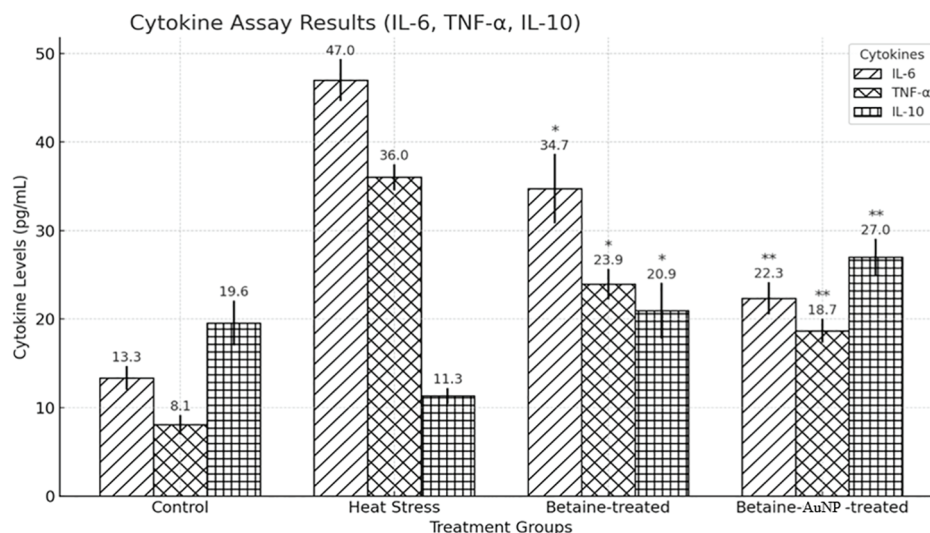

Chart 1. Cytokine Analysis (IL-6, TNF-α, IL-10): The cytokine measurements revealed significant variations, as depicted with error bars. IL-6 and TNF-α concentrations were marked with asterisks to indicate significant differences: A notable reduction in IL-6 was observed between the Control and Heat Stress groups. Similarly, a marked decrease in TNF-α was evident between the Heat Stress group and the Betaine-AuNPs-treated group. Statistical significance is denoted as follows: * indicates a significant difference ($p<0.05$), while ** denotes a highly significant difference ($p<0.01$), comparing Betaine-treated and Betaine+AuNPs-treated groups to the Heat Stress group.

Heat Shock Protein (HSP70) Expression

HSP70, a critical marker of cellular stress, exhibited a pronounced increase in the Heat Stress group as a direct response to elevated temperatures (15). Conversely, the Betaine-AuNPs-treated group displayed a significant reduction in HSP70 expression compared to the untreated heat-stressed group. These findings demonstrate the efficacy of AuNPs and betaine in mitigating cellular stress (Chart 2).
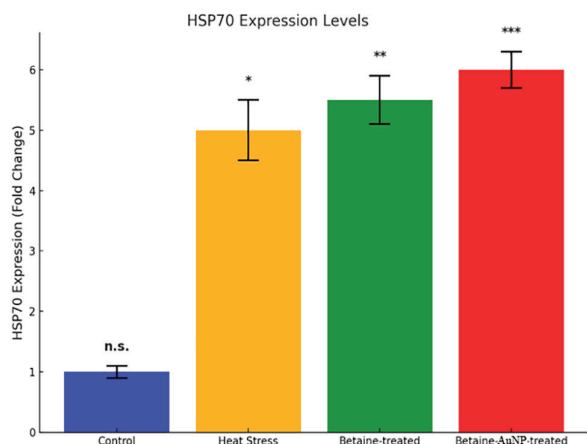
Chart 2. Heat Shock Protein (HSP70) Expression: HSP70 expression levels are illustrated with error bars and significance indicators for each experimental group. Significance levels are denoted as follows: n.s. (not significant) for the Control group, * (p<0.05) for the Heat Stress group, and ** (p<0.01) for the Betaine-treated group.
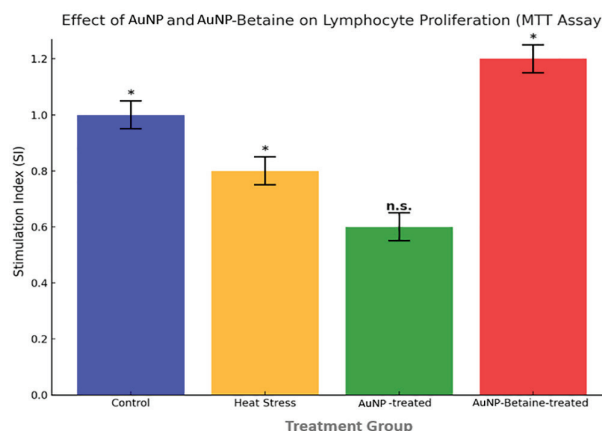

Chart 3. MTT assay results illustrating the effect of AuNP and AuNP-Betaine on lymphocyte proliferation. The stimulation index (SI) was calculated by dividing the absorbance of stimulated cells by that of unstimulated cells. Error bars represent standard deviation (SD). A single asterisk (*) indicates statistical significance (p<0.05), and two asterisks (**) denote highly significant differences (p<0.01) compared to the control group.

MTT Test Outcomes

The MTT test is employed to study cellular growth rates under various conditions, including control, stress, and treatment groups. A higher rate of proliferation results in greater conversion of MTT to formazan. In the control group, the Stimulation Index (SI) was 1.0, which served as the baseline for comparison and showed significant differences (*) when compared to all other groups.

In the Heat Stress Group, the SI declined to approximately 0.8, demonstrating a significant reduction (*) compared to the control group. This result indicates the adverse impact of heat stress on lymphocyte proliferation. The AuNP-Treated Group exhibited a further decline in SI to approximately 0.6, underscoring the detrimental effects of AuNP treatment on lymphocyte proliferation. However, this reduction was not statistically significant (n.s.) compared to the Heat Stress group, indicating similar levels of suppression in both cases.

The findings from the MTT assay demonstrate that both heat stress and AuNP treatments exert cytotoxic effects on lymphocytes, as reflected by

reduced Stimulation Index (SI) values compared to the control group (SI ≈ 1.0). Heat stress alone induced a moderate decrease in lymphocyte proliferation (SI ≈ 0.8), while AuNP treatment led to a further decline (SI ≈ 0.6), indicating substantial cytotoxicity, presumably due to AuNP interactions with cellular processes. However, the conjugation of AuNPs with betaine resulted in the mitigation of cytotoxic effects, whereby lymphocyte proliferation not only recovered but exceeded baseline levels (SI ≈ 1.2). This observation suggests that betaine confers a protective effect, thereby neutralizing the detrimental impact of AuNPs and promoting enhanced cell viability and growth.

Notably, in the AuNP-Betaine-Treated Group, the SI dramatically increased to 1.2, which was significantly (*) higher than all other groups, including the control group. This finding indicates that the addition of betaine not only neutralized the negative effects of AuNP but also significantly enhanced lymphocyte proliferation beyond the baseline level. Furthermore, the AuNP-Betaine-treated group demonstrated a remarkable enhancement in lymphocyte growth

326

compared to the AuNP-only group, suggesting that betaine attachment effectively reversed the detrimental impacts of AuNPs, thereby restoring and even boosting cell proliferation beyond control levels (Chart 3).

Discussion

The findings of this research demonstrate that AuNP-betaine conjugates play a crucial role in diminishing heatstroke-related inflammation, which constitutes a major factor contributing to organ dysfunction during heatstroke (16). What is particularly noteworthy is the significant reduction in pro-inflammatory cytokines such as TNF-α and IL-6 in the AuNP-betaine-treated group compared to untreated mice, which underscores the potential of AuNPs to serve as effective nanocarriers for delivering anti-inflammatory agents like betaine to inflamed tissues. This observation aligns with prior studies emphasizing the promise of nanotechnology in enhancing the effectiveness of bioactive compounds.

In support of these findings, research by Uchiyama et al. (2014) demonstrated that gold nanoparticles conjugated with anti-inflammatory agents significantly reduced inflammation and promoted tissue repair in a mouse model of acute inflammation (17). Moreover, AuNPs have been demonstrated to improve the stability and targeted delivery of bioactive molecules to inflamed sites, which corroborates our observations (18).

The enhanced therapeutic outcomes observed in the AuNP-betaine-treated group can be attributed to the synergistic effects between betaine and AuNPs. While betaine is well-known for its ability to reduce inflammation by lowering levels of pro-inflammatory cytokines, its conjugation with AuNPs significantly enhances its bioavailability and precise delivery to the targeted sites, thereby resulting in increased therapeutic efficacy. This synergistic interaction corresponds with findings by Zhang et al. (2020), who reported that combining functionalized gold nanoparticles

with natural antioxidants improved therapeutic outcomes in oxidative stress models (19). These observations collectively highlight the dual role of AuNP-betaine conjugates in providing both enhanced stability and targeted action.

Of particular significance is the substantial increase in HSP70 expression observed in the AuNP-betaine-treated group compared to the untreated heat-stressed group, which indicates a reduction in cellular stress (20, 21). Heat shock proteins, particularly HSP70, are instrumental in protecting cells against stress by preventing protein misfolding and supporting cellular stability during elevated temperature conditions (15). Previous research has demonstrated that exposure to heat stress significantly increases HSP70 levels, representing a protective mechanism to combat cellular damage. It has been established that interventions like betaine can further enhance this response, as it acts as a stabilizer of proteins and cellular frameworks under stress conditions (22).

The mechanism through which betaine's methyl donor properties contribute to this process likely involves the modulation of cellular inflammation, inhibition of pro-inflammatory cytokines, and enhancement of membrane stability (23). What makes this intervention particularly effective is that when combined with AuNPs, this anti-inflammatory and stress-mitigating capacity is amplified due to the nanoparticle's ability to enhance the stability, availability, and cellular uptake of betaine (24).

Similar studies have corroborated the role of AuNPs in enhancing the activity and effectiveness of natural compounds (25-27). Furthermore, animal studies have consistently demonstrated that betaine administration results in an upregulation of HSP70 levels, thereby increasing resilience to environmental stressors, including heat stress (28). Recent investigations suggest that AuNPs associated with bioactive compounds like betaine can further enhance heat shock protein activity by improving their

Loghmani A, et al

bioavailability and cellular uptake (29, 30). It is this synergy that may explain the significant rise in HSP70 levels observed in this study, thereby providing enhanced cellular protection under heat stress conditions (31).

The MTT assay results further substantiate the positive effects of AuNP-betaine conjugates on immune functionality. What is particularly noteworthy is the increase in lymphocyte proliferation in the AuNP-betaine-treated group, which indicates that these conjugates not only reduce inflammation but also restore immune cell activity, which typically becomes suppressed during heat-related ailments (32). Numerous studies have demonstrated that gold nanoparticles possess inherent anti-inflammatory properties, which likely contribute to the therapeutic outcomes observed in this study (33, 34).

The efficacy of betaine in reducing inflammation extends beyond heatstroke models. For instance, research by Arumugam et al. (2022) demonstrated that betaine reduced oxidative damage associated with alcohol-induced liver injury through its antioxidant mechanisms (35). In our study, the combination of AuNPs and betaine demonstrates the therapeutic potential of leveraging their complementary properties. Due to their high surface area-to-volume ratio, AUNPs effectively carry and deliver betaine to target cells, thereby enhancing its cellular absorption and internal concentration (36).

Moreover, conjugation with AuNPs protects betaine from rapid enzymatic degradation, thus prolonging its circulation time and ensuring sustained therapeutic effects. Current research indicates that enzymes adsorbed onto nanoparticles exhibit increased stability and resistance to denaturation (37), suggesting comparable benefits for biomolecules like betaine. Beyond improving stability, AuNP-betaine conjugates enhance betaine's ability to block inflammatory pathways such as NF-κB, which serves as a key mediator in chronic inflammation (38). This controlled-release mechanism maintains betaine's therapeutic concentration over time, thereby amplifying its effects on inflammatory processes (39). These findings align with recent advancements in nanomedicine that emphasize precise drug delivery and synergistic treatment approaches for inflammatory diseases (40).

Conclusion

While our findings are promising, it is imperative to address the challenges associated with AuNP-betaine conjugates and detailed *in vivo* studies are required to elucidate the pharmacokinetics, long-term distribution, and potential adverse effects of AuNPs prior to enter into clinical applications. Furthermore, the scalability of nanoparticle production and its associated costs remain significant barriers to clinical translation. It is crucial to ensure cost-effectiveness and maintain quality control during large-scale production for the successful implementation of this technology.

Acknowledgments

Conflicts of interest

The authors declare no conflicts of interest related to this work.

Funding

Ethical Considrations

All animal experiments were conducted in accordance with ethical standards for the maintenance and use of laboratory animals. The Animal Ethics Committee of the University of Lorestan reviewed and approved the study

protocol (Protocol No. B0254), ensuring compliance with national and international standards for the humane treatment of animals in research.

Code of Ethices

The Animal Ethics Committee of the University of Lorestan approved the study protocol under Protocol No. B0254.

Authors' Contributions

All authors contributed equally to this study.

References

1 Ravindra K, Bhardwaj S, Ram C, Goyal A, Singh V, Venkataraman C, et al. Temperature projections and heatwave attribution scenarios over India: A systematic review. *Heliyon*. 2024;10(4):26431.

2 Manivannan A, Kabbani D, Levine D. Use of multiple anticholinergic medications can predispose patients to severe non-exertional hyperthermia. *BMJ Case Rep.* 2021;14(3): 2398-05.

3 Wang F, Zhang Y, Li J, Xia H, Zhang D, Yao S. The pathogenesis and therapeutic strategies of heat stroke-induced liver injury. *Crit Care*. 2022;26(1):391.

4 Iba T, Connors JM, Levi M, Levy JH. Heatstroke-induced coagulopathy: Biomarkers, mechanistic insights, and patient management. *EClinMed*. 2022;44(5):1012-76.

5 Sun M, Li Q, Zou Z, Liu J, Gu Z, Li L. The mechanisms behind heatstroke-induced intestinal damage. *Cell Death Discov*. 2024;10(1):455.

6 Zhou X, Wei C, Chen Z, Xia X, Wang L, Li X. Potential mechanisms of ischemic stroke induced by heat exposure. *Sci Total Environ*. 2024;952(12):1758-65.

7 Karnwal A, Kumar Sachan RS, Devgon I, Devgon J, Pant G, Panchpuri M, et al. Gold nanoparticles in nanobiotechnology: From synthesis to biosensing applications. *ACS Omega*. 2024;9(28):29966–82.

8 Dreaden EC, Austin LA, Mackey MA, El-Sayed MA. Size matters: Gold nanoparticles in targeted cancer drug delivery. *Ther Deliv*. 2012;3(4):457–78.

9 Aili M, Zhou K, Zhan J, Zheng H, Luo F. Anti-inflammatory role of gold nanoparticles in the prevention and treatment of Alzheimer's disease. *J Mater Chem B*. 2023;11(36):8605–21.

10 Cao F, Gui S-Y, Gao X, Zhang W, Fu Z-Y, Tao L-M, et al. Research progress of natural product-based nanomaterials for the treatment of inflammation-related diseases. *Mater Des*. 2022;218(3):110686-95.

11 Arumugam MK, Paal MC, Donohue TM, Ganesan M, Osna NA, Kharbanda KK. Beneficial effects of betaine: A comprehensive review. *Biol*. 2021;10(6):456.

12 Zarenezhad E, Abdulabbas HT, Marzi M, Ghazy E, Ekrahi M, Pezeshki B, et al. Nickel Nanoparticles: Applications and antimicrobial role against Methicillin-Resistant Staphylococcus aureus infections. Antibiotics. 2022;11(9):1208.

13 Sharma HS. Methods to produce hyperthermia-induced brain dysfunction. In: Sharma HS, editor. *Progress in Brain Research*. Elsevier;. (Neuro Hyper. 2007; 162(3):127-35.

14 Gong T-W, Fairfield DA, Fullarton L, Dolan DF, Altschuler RA, Kohrman DC, et al. Induction of heat shock proteins by hyperthermia and noise overstimulation in hsf1 −/− mice. *JARO*. 2012;13(1):29–37.

15 Rosic NN, Pernice M, Dove S, Dunn S, Hoegh-Guldberg O. Gene expression profiles of cytosolic heat shock proteins Hsp70 and Hsp90 from symbiotic dinoflagellates in response to thermal stress: Possible implications for coral bleaching. *Cell Stress Chaperones*. 2011;16(1):69–80.

16 Heled Y, Fleischmann C, Epstein Y. Cytokines and their role in hyperthermia and heat stroke. *J Basic Clin Physiol Pharmacol*. 2013;24(2):85–96.

17 Uchiyama MK, Deda DK, Rodrigues SFDP, Drewes CC, Bolonheis SM, Kiyohara PK, et al. In vivo and in vitro toxicity and anti-inflammatory properties of gold nanoparticle bioconjugates to the vascular system. *Toxicol Sci*. 2014;142(2):497–507.

18 Hu X, Zhang Y, Ding T, Liu J, Zhao H. Multifunctional gold nanoparticles: A novel nanomaterial for various medical applications and biological activities. *Front Bioeng Biotechnol*. 2020;8(2):990-98.

19 Zhang X, Guo X, Kang X, Yang H, Guo W, Guan L, et al. Surface functionalization of pegylated gold nanoparticles with antioxidants suppresses nanoparticle-induced oxidative stress and neurotoxicity. *Chem Res Toxicol*. 2020;33(5):1195–205.

20 Lee WC, Wen HC, Chang CP, Chen MY, Lin MT. Heat shock protein 72 overexpression protects against hyperthermia, circulatory shock, and cerebral ischemia during heatstroke. *J Appl Physiol*. 2006;100(6):2073–82.

21 Dineen SM, Ward JA, Plamper ML, Mayer TA, Leon LR. An increase in thermotolerance is associated with elevated levels of heat shock protein 70 (Hsp70) in a mouse exertional heat stroke model. *FASEB J*. 2020;34(2):1–17.

22 Willingham BD, Ragland TJ, Ormsbee MJ. Beta-ine supplementation may improve heat toler-ance: Potential mechanisms in humans. *Nutrients*. 2020;12(10):29-39.

23 Saleh, A. A., El-Tahan, H. M., Shaban, M., Morsy, W. A., Genedy, S., Alzawqari, M. H., et al. Serum biochemical parameters, nutrients digestibility, and growth-related genes in broilers under heat stress. *Poultry Science*. 2023 *102*(11), 103051.

24 Sridhar K, Inbaraj BS, Chen B-H. Recent advances on nanoparticle based strategies for improving carotenoid stability and biological activity. *Antioxi-dants*. 2021;10(5):713-25.

25 Khandanlou R, Murthy V, Wang H. Gold nanopar-ticle-assisted enhancement in bioactive properties of Australian native plant extracts, Tasmannia lan-ceolata and Backhousia citriodora. *Mater Sci Eng C*. 2020;112(5):110-22.

26 Abdellatif AA, Ahmed F, Mohammed AM, Alshari-dah M, Al-Subaiyel A, Samman WA, et al. Recent advances in the pharmaceutical and biomedical applications of cyclodextrin-capped gold nanopar-ticles. *IJN*. 2023;18(32):47–81.

27 Gangwar RK, Dhumale VA, Kumari D, Nakate UT, Gosavi SW, Sharma RB, et al. Conjugation of curcumin with PVP capped gold nanoparticles for improving bioavailability. *Mater Sci Eng C*. 2012;32(8):2659–63.

28 Alagawany M, Elnesr SS, Farag MR, El-Naggar K, Taha AE, Khafaga AF, et al. Betaine and related compounds: Chemistry, metabolism and role in mitigating heat stress in poultry. *J Therm Biol*. 2022;104(3):1030-38.

29 Uyanga VA, Oke EO, Amevor FK, Zhao J, Wang X, Jiao H, et al. Functional roles of taurine, L-theanine, L-citrulline, and betaine during heat stress in poul-try. *J Anim Sci Biotechnol*. 2022;13(1):23.

30 Sun S, Yin Q, Li B, Deng Y, Li J, Xiong Y, et al. Effects of betaine on viability, apoptosis, func-tion protein expression and oxidative status in heat-stressed iec-6 cells. *SSRN J*. 2022;126(5):56-62

31 Ibrahim B, Akere TH, Chakraborty S, Valsami-Jones E, Ali-Boucetta H. Modulation of heat shock protein expression in alveolar adenocarcinoma cells through gold nanoparticles and cisplatin treatment. *Pharmaceutics*. 2024;16(3):380-87.

32 Cantet JM, Yu Z, Ríus AG. Heat stress-mediated activation of immune–inflammatory pathways. *Antibiotics*. 2021;10(11):1285-93.

33 De Araújo RF, De Araújo AA, Pessoa JB, Freire Neto FP, Da Silva GR, Leitão Oliveira ALCS, et al. Anti-inflammatory, analgesic and anti-tumor properties of gold nanoparticles. *Pharmacol Rep*. 2017;69(1):119–29.

34 Blaney C, Sommer J, El-Gabalawy R, Bernstein C, Walld R, Hitchon C, et al. Incidence and temporal trends of co-occurring personality disorder diag-noses in immune-mediated inflammatory diseases. *Epidemiol Psychiatr Sci*. 2020;29(5):70-84.

35 Arumugam MK, Chava S, Perumal SK, Paal MC, Rasineni K, Ganesan M, et al. Acute ethanol-induced liver injury is prevented by betaine admin-istration. *Front Physiol*. 2022;13(2):9401-15.

36 Alsaidan OA. Nanocarriers: Exploring the potential of oligonucleotide delivery. *CDD*. 2024;21(6):91-01

37 Tripathi S, Siddiqui MH, Kumar A, Vimal A. Nanoparticles: A promising vehicle for the delivery of therapeutic enzymes. *Int Nano Lett*. 2023;13(4):209–21.

38 Xia Y, Chen S, Zhu G, Huang R, Yin Y, Ren W. Betaine inhibits interleukin-1β production and release: Potential mechanisms. *Front Immunol*. 2018;9(3):26-40.

39 Wang C, Ma C, Gong L, Dai S, Li Y. Preventive and therapeutic role of betaine in liver disease: A review on molecular mechanisms. *Eur J Pharmacol*. 2021;912(6):1746-54.

40 Yetisgin AA, Cetinel S, Zuvin M, Kosar A, Kutlu O. Therapeutic nanoparticles and their targeted deliv-ery applications. *Molecules*. 2020;25(9):2193.